LA-UR-95- 4385

CONF-960202--3

RECEIVED

FEB 15 1996

OSTI

Los Alamos National Laboratory is operated by the University of California for the United States Department of Energy under contract W-7405-ENG-36.

TITLE: Modeling of Ductile and Brittle/Brittle Laminates

Atuhors Shao-:Ping Chen, T-11

SUBMITTED TO: "Modeling of Compsites: processing and dprperties", Ed. by S.P. Chen and M.P. Anderson, 1996 The minerals, metals and materials Society Meeting. Anaheim, CA Feb 4-8, 1996

Los Alamos National Laboratory
Los Alamos, New Mexico 87545

FORM NO. 836 R4
ST. NO. 2629 5/81

MODELING OF DUCTILE AND BRITTLE/BRITTLE LAMINATES

S. P. Chen

Theoretical Division, Los Alamos National Laboratory,
Los Alamos, New Mexico 87545, USA

Abstract

A micro-mechanical "spring"-network model was used to simulate the deformation and fracture behaviors of ductile/brittle and brittle/brittle laminates. The effects of the interfacial cohesion, moduli, grain boundary cohesion, yield stress are presented and compared with available experiments. We found that composites with higher yield stress and lower interfacial cohesion are tougher.

Introduction

We make composites to utilize the various properties of the constituent materials and to optimize the required physical, mechanical and thermodynamic properties [1, 2]. The fact that brittle solids as well as ductile materials can be toughened by brittle materials was demonstrated by Prewo and Brennan in 1982 [3] and some later developments have been summarized by Evans [2]. Quite significant progress has been made in the area of the modulus dependence on the volume fractions, moduli, sizes, and thicknesses of the fibers and laminates [2, 3]. Many models, such as the Shear-lag, Laminated plate, Eshelby and finite element methods have been applied to understand the mechanical properties of the composites with reasonable success [4, 5]. But a clear understanding of how the interfaces control the properties of the composite is still needed. We present here the simulation results obtained from a "spring"-network model for the mechanical properties of the composites. Good agreement with available data and previous theories was obtained.

Calculation Procedure

The "spring"-network model used here has been described and discussed before [6-10]: we only briefly summarize it here. The model consists of a 2-dimensional "spring" network on a triangular lattice. The laminate 1 (the white phase in Fig. 3) is composed of multi-grained materials which is brittle (grain boundaries are represented as thin lines), while laminate 2 (the light gray area) is treated as a uniform material which can be brittle or ductile. The simulations are performed on a 50x50, 100x100 or 150x150 nodes cell which is periodic in the x-direction and free in the y-direction. The nodes are connected with linear springs that obey Hooke's law: $F=k(r-r_0)$, where F is the force, k is the spring constant, r is the length of the spring and r_0 is the length of the original spring. For the brittle/brittle laminates, the bulk springs break at a strain of 0.005 and the grain boundaries break at a strain of 0.003. For the ductile phase, the "spring" is described by a elastic, perfectly plastic stress-strain behavior as shown in Fig.1. The choice of these parameters ensure a proper mix of intergranular and transgranular fractures as shown in Fig. 2 [6]. The interface springs are chosen to break at strains from 0.001 to 0.007. Because the energy associated with the spring is quadratic in the strain, therefore the resulting relative interfacial cohesion energy with respect to the matrix, Γ_i/Γ_f, is varied from 0.04 to 1.96. This range of Γ_i/Γ_f is chosen to test the important effects of the interfacial debonding and fiber cracking regimes as predicted by He and Hutchinson and others [11, 12]. The elastic moduli (and thus the spring constants) for laminates 1 and 2

are the same, which corresponds closely to $MoSi_2/Al_2O_3$ composites or other metals/ceramics composites that have similar elastic constants (with k=1.0). The relative portion of these two laminates is kept at a 1:1 ratio and each phase is 5-layer thick. In this simulation, the change of the fracture behaviors are purely due to the change of the interfacial cohesion, Γ_i/Γ_f. A 2x10 nodes of pre-crack is introduced at the bottom of the cell (dark gray area) in the beginning and the system is stretched in the x-direction by a strain step of 0.0001 and relaxed to the minimum energy by either moving the nodes or cracking the springs if the spring

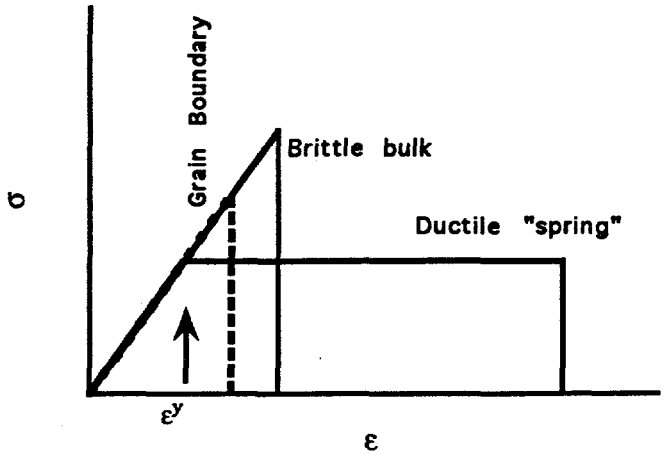

Fig. 1 The stress-strain curves of the ductile, brittle bulk and grain boundary "springs".

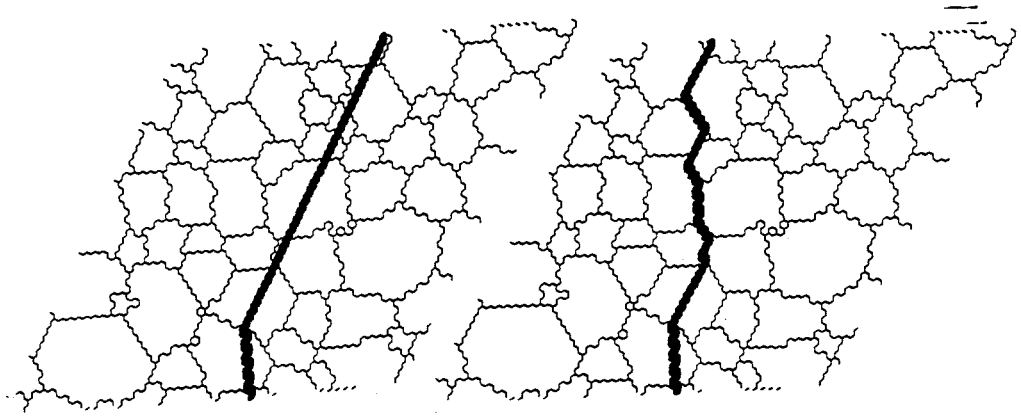

Fig. 2 (a) The polycrystals break intergranularly when the breaking strengths of the bulk and grain boundary are the same. (b) The polycrystals break both transgranularly and intergranularly when the grain boundary strength is lower than (36%) the bulk strength.

reaches the breaking strain (and Γ_i/Γ_f). The strain was applied 50 times to reach the strain level of 0.005 for the brittle/brittle case. For the ductile/brittle laminates, the strain was applied until the composites fail.

Brittle/Brittle Laminates

The fracture paths of representative laminates with weak and strong interfaces are presented in Fig. 3a and 3b, respectively. We found that the fracture paths of these laminates are more zig-zagged and numerous for composites with weak interfaces than for the composites with strong interfaces. Also the widths of the cracks are wider for weak interfaces: therefore, the composites with weak cohesion at the interfaces debond at interfaces (Fig. 3a). These debondings at the interfaces relieve the stress ahead of the crack and thus shield the crack and toughen the composites. For composites with strong interfaces, the crack runs straight through the laminates as if the interfaces do not exist at all (Fig. 3b). These fracture behaviors are found to be similar for fibers, particulates and laminate enforcement of brittle/brittle composites [2]. These toughening effects observed for the composites with weak interfaces agree with the experiments for glass/C/SiC (weak) interfaces and glass/SiO_2/SiC (strong) interfaces [2, 13-15] as well as for many $MoSi_2/Al_2O_3$ interfaces that stay intact for clean (and presumably strong) interfaces but debond at the Al_2O_3 interfaces when amorphous (and weak) phases are present at the interfaces [16]. We also found that as the interfacial cohesions, Γ_i/Γ_f, are lowered, the cracks start to be deflected first singly and then doubly as demonstrated theoretically by many [11, 12].

The calculated stress-strain curves corresponding to the composites of Fig. 3 are shown in Fig. 4. The solid curve in Fig. 4 corresponds to a composite with low interfacial cohesion (Fig. 3a), with Γ_i/Γ_f =0.04, that shows a typical 'tough' composite curve [2] with a distinctive interfacial cracking point at I and changes to a smaller slope at II, fractures extensively at III and fractures completely at IV. The normalized fracture energy, W, with respect to the pure multi-grained materials of laminate 1 [6-8] as measured by the area under the stress-strain curve is 2.9. This value is significantly larger than the original matrix, the ultimate tensile stress, σ_u, is higher by about 50%, and the fracture strain is about 130% higher too. The fracture paths with extensive interfaces debondings in this composite are shown in Fig. 3a. This extensive cracking can also be observed by the number of bonds broken as a function of the Γ_i/Γ_f [8]. Effectively, the extensive cracks blunt the main crack and relieve the stress ahead of the crack: therefore, the laminates

are tougher. This extensive cracking at the interfaces may be undesirable if the oxidation resistance, air or fluid leakage, environmental stability and creep resistance is crucial to the application. For laminates with high interfacial cohesion, with Γ_i/Γ_f = 0.81, the stress-strain curve (the dashed line in Fig. 4) shows a typical 'brittle' composite behavior by having a linear dependence on strain up to the final fracture strain with a single dominant fatal crack running through all the laminates without debonding at the interfaces. The matrix cracking stress, σ_0 (0.96 of σ_u), is almost the same as the ultimate tensile stress, σ_u. Both σ_u and σ_0 are exactly the same as that of the pure matrix material. No toughening or strengthening was derived from the laminates with high interfacial cohesion ($\Gamma_i/\Gamma_f > 0.6$). The trends of σ_u and σ_0 as a function of the interfacial cohesion are totally consistent with the results on LAS glass matrix and SiC (Nicalon) fibers with variable amounts of C or SiO_2 at the interfaces to control the interfacial cohesions [2, 13-15].

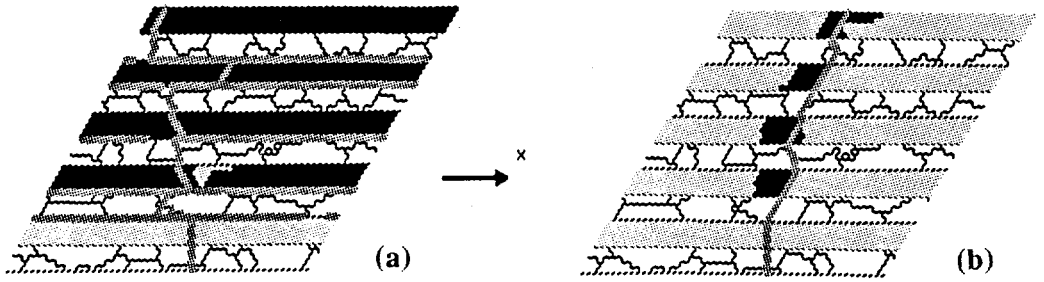

Fig. 3: (a) The fracture paths of brittle/brittle laminates with Γ_i/Γ_f=0.04 and (b) Γ_i/Γ_f=0.81. The solid black area (only shown for laminate 2) is the high-stressed area that is at the level of macroscopic fracture of matrix material, the dark gray area is the crack, the light gray area is the laminate 2, the white area is laminate 1 and the thin line is the grain boundary.

The normalized fracture energy, W, as a function of the interfacial cohesion, Γ_i/Γ_f, is plotted in Fig. 3a. First, we found that none of the laminates are weakened with the introduction of either strong or weak interfaces. We found that the laminates with good cohesion (with $\Gamma_i/\Gamma_f >$ 0.6) are not toughened with the introduction of these extra interfaces. These extra interfaces have effects in toughening only when the

interfacial cohesion is below 0.6. The toughening is due to the arrest of the crack at the interfaces with some small scale blunting, which is accompanied by a different fracture path [8]. This toughening is due to the fact that no weak fracture paths can be found nearby and higher stresses are needed to drive the crack through the laminates which is accompanied with only a small amount of interfacial debonding. This toughening effect diminishes as the interfacial cohesion decreases further till the value of 0.4 is reached, whereupon extensive crackings occur and thus significantly relieve the stresses of the main crack. The rise of W for composites with interfacial cohesion from 0.41 to 0.4 is rather rapid which indicates a drastic change of mechanism for the fracture process. This is mainly due to the debonding at the interfaces (Fig. 3a and 3b). This Γ_i/Γ_f value of 0.4 is also coincident with the propensity of grain boundary fracture (a special case of interfacial cracking) as shown in Fig. 5 for many metals and intermetallic compounds [17].

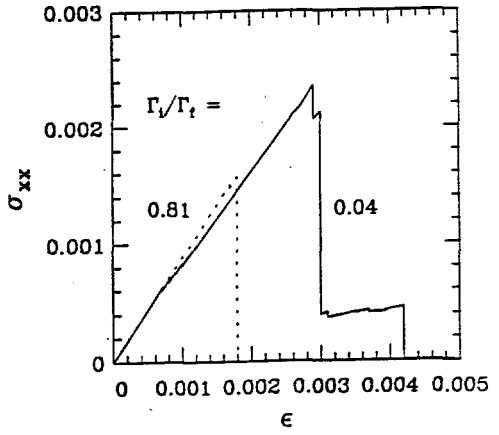

Fig. 4 The stress-strain curves corresponding to Fig. 3a and 3b.

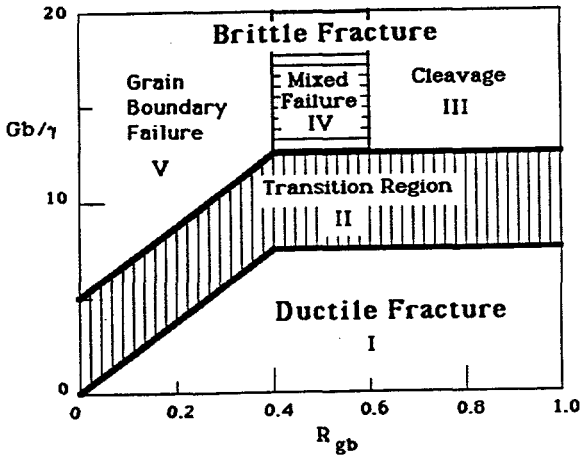

Fig. 5 The intrinsic grain boundary (or interfacial) fracture map divides materials into five regions of fracture behaviors based on their values of Gb/Γ and R_{gb} (= Γ_i/Γ_f). Where, G is the shear modulus, b is the Burger's vector, Γ is the surface energy, R_{gb} is the relative grain boundary (interfacial) cohesion (=Γ_i/Γ_f). From [17].

The enhancement of the normalized fracture energy can be **crudely** approximated by the following formula (also shown in Fig. 6a):

$$W = W_0 - A\,\Gamma_i/\Gamma_f, \quad \text{where } W_0=2.9 \text{ and } A=3.1 \qquad \text{for } \Gamma_i/\Gamma_f < 0.6;$$

$$= 1.0 \qquad \text{for } \Gamma_i/\Gamma_f > 0.6 \qquad (1)$$

The dependence of the normalized ultimate tensile stress, σ_u, as a function of the interfacial cohesion, Γ_i/Γ_f, is plotted in Fig. 6b. The σ_u stays flat for Γ_i/Γ_f above 0.4 and suddenly jumps up 27% when Γ_i/Γ_f goes below 0.4 and then continuously goes up as a linear function of $-\Gamma_i/\Gamma_f$. The reason for this strengthening is the same as for the toughening, namely the main crack has been shielded by the interface debonding. The higher value of 0.4 for the interfacial cohesion as compared to the value of 0.25 of He and Hutchinson [11] is due to the multi-laminates used here instead of the composite with a single interface treated in He and Hutchinson [11]. With one single interface, we have reproduced their result of 0.25 perfectly [8]. A **crude** formula can be written as:

$$\sigma_u = 1.51 - 0.83\,\Gamma_i/\Gamma_f, \qquad \text{for } \Gamma_i/\Gamma_f < 0.4;$$

$$= 1.0 \qquad \text{for } \Gamma_i/\Gamma_f > 0.4 \qquad (2)$$

The relative initial cracking stress, σ_0, of these laminates is also plotted as a function of the interfacial cohesion in Fig. 6b. We found that as the Γ_i/Γ_f is lowered the interfaces debond (Fig. 3a) and σ_0 is lowered. This is opposite to the trend for the ultimate tensile stress, σ_u. The drop of the σ_0 as Γ_i/Γ_f is lowered is much faster than the rise of the σ_u. The σ_o for Γ_i/Γ_f=0.04 is only 40% of the initial cracking stress of the original matrix. The dependence of the relative initial cracking stress as a function of Γ_i/Γ_f can be described as:

$$\sigma_0 = 0.38 + 1.79\,\Gamma_i/\Gamma_f, \qquad \text{for } \Gamma_i/\Gamma_f < 0.4;$$

$$= 0.96 \qquad \text{for } \Gamma_i/\Gamma_f > 0.4 \qquad (3)$$

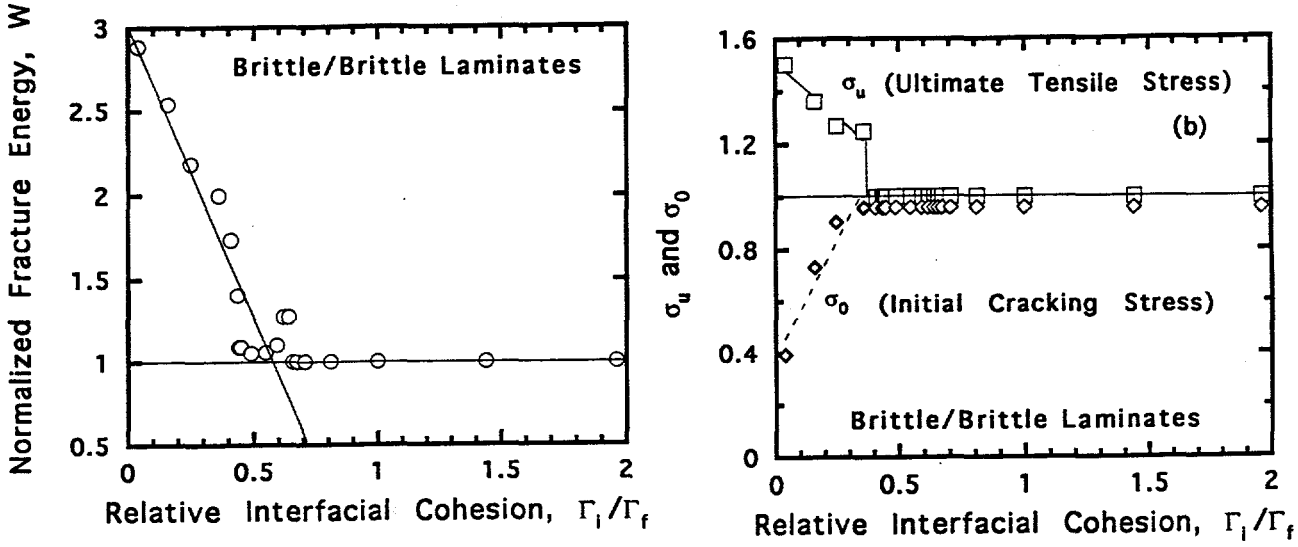

Fig. 6(a): The relative fracture energy, W, plotted as a function of the interfacial cohesion, Γ_i/Γ_f. (b) The relative ultimate tensile stress, σ_u, and the initial cracking stress, σ_0, plotted as a function of the interfacial cohesion.

Ductile/Brittle Laminates

For the ductile/brittle laminates, we found that the composites break before the breaking strain of the laminate 2 is achieved. This is due to the confinement of the ductile phase that makes the composite easier to break than in a pure bulk form. This result is consistent with what was observed experimentally for metal composites [2]. The total fracture energy as measured by the area under the stress-strain curve, Fig. 7a, is roughly linear in the yield strain (Fig. 7b).

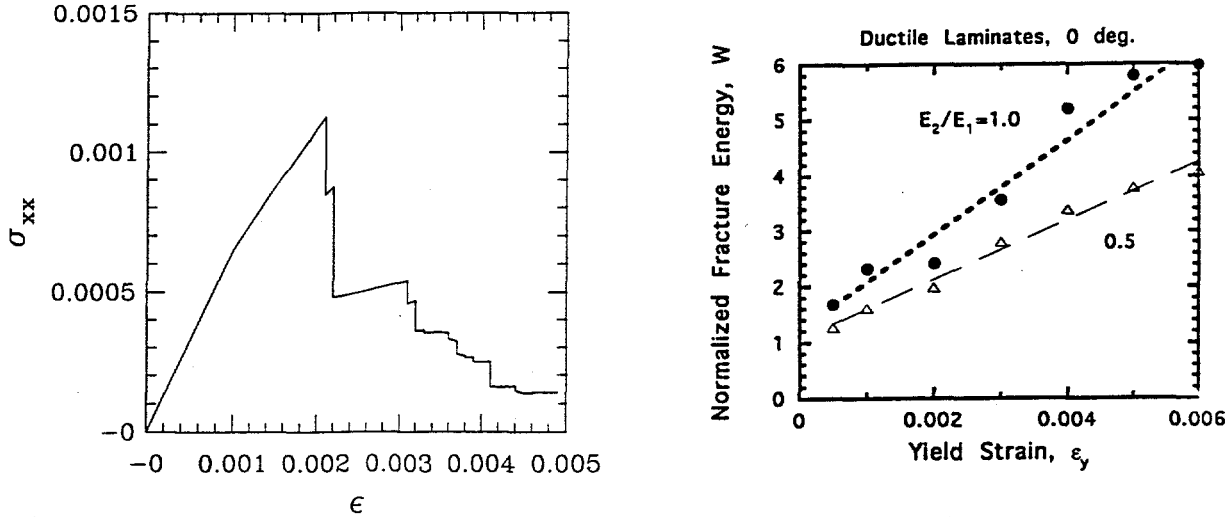

Fig. 7 (a) The stress-strain curve for the ductile/brittle laminates. Region I is elastic, II is plastic, III is micro-cracking in brittle laminate 1, IV is elastic and plastic again. (b) The normalized fracture energy as a function of the yield strain (or stress as indicated in Fig. 1).

The interfacial cohesion has significant effects on the deformation and fracture behavior similar to the brittle/brittle laminates as shown in Fig. 8. When the interfacial cohesion is low, the deformation is dominated by interfacial delamination and extensive plastic deformation (as indicated by the solid black regions). The toughening is the greatest (Fig. 8a and b). As the interfacial cohesion increases, the interfacial delaminations as well as plastic deformations decrease and one major crack develops (Fig. 8c). As the interfacial cohesion further increases, the plastic zone sizes increase and the toughening increase modestly with lots of tunnel cracks in the brittle laminate 1 (Fig. 8d). The normalized work of fracture are

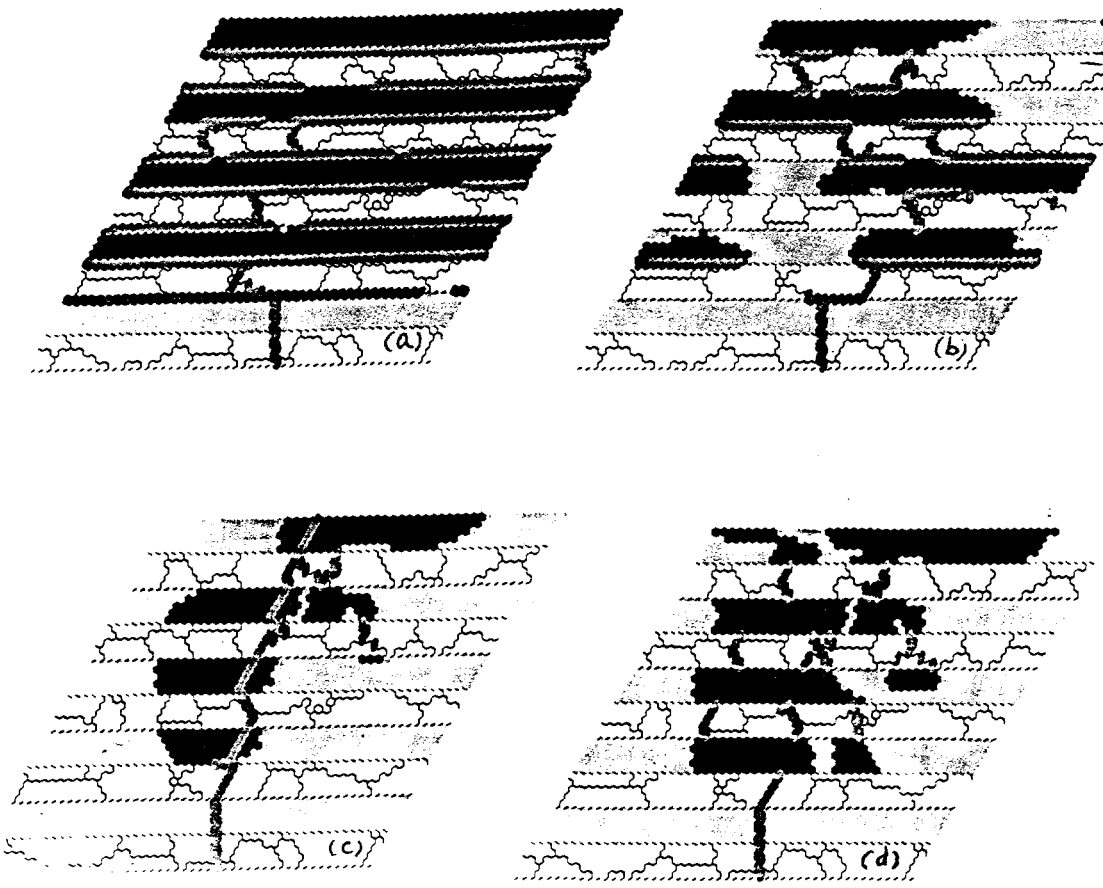

Fig. 8 (a) and (b) Ductile/brittle laminates with weak interfaces, (c) with medium interfaces, and (d) strong interfaces.

shown in Fig. 9a. The work of fracture for the strong interfaces are about twice higher than the brittle/brittle laminates due to the contribution of the platic work. This level is found to be a linear function of the yield stress as indicated in Fig. 7b. The ultimate tensile stress (σ_u) and initial cracking stresses (σ_0) as a function of the interfacial cohesion are also shown in Fig. 9b. The qualitative trends for both σ_u and σ_0 are similar to the brittle/brittle laminates. For very weak interfaces, the maximum value of σ_u (1.25) is smaller, while the minimum value for σ_0 (0.2) is lower than the corresponding case in brittle/brittle case.

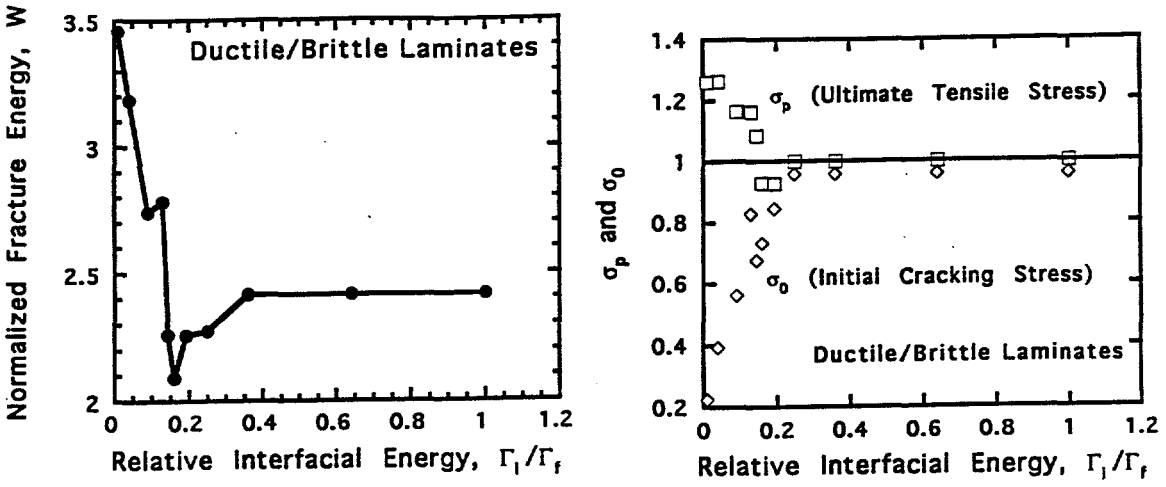

Fig. 9 (a) The normalized work of fracture as a function of interfacial cohesion. A surprising dip was found for medium interfacial cohesion (see Fig. 8c). (b) The σ_u and σ_0 as a function of interfacial cohesion.

Conclusions

Using the "spring"-network model, we found that both the brittle/brittle and ductile/brittle laminates with weak interfaces can be stronger and tougher mechanically. The fracture paths and the stress-strain curve obtained here are consistent with available experiments and theories. The fracture behaviors, fracture energies (W), ultimate tensile stresses (σ_u) and the initial cracking stress (σ_0) have been studied as a function of the relative interfacial cohesion, Γ_i/Γ_f, of the laminates. These toughening and strengthening effects are due to the extensive debonding (and plastic deformations) at the interfaces which act to shield the main crack. A surprising dip in the work of fracture was found when the interfacial cohesion is of medium value. The detailed mechanism of this phenomenon needs to be explored further. The understanding and the quantitative formula derived from these simulations can be used to

design tougher and stronger composites by proper control of the interfacial cohesion and yield stress.

Acknowledgment

We would like to acknowledge the support of the U. S. Department of Energy.

References

1. M. F. Ashby, Acta Met. et Mat., **41**, 1313 (1993) and references cited therein.
2. A. G. Evans, J. Am. Ceram. Soc., **73**, 187 (1990) and references cited therein.
3. K. M. Prewo and J. J. Brennan, J. Mater. Sci., **17**, 1201 (1982).
4. T. Mura, "Micromechanics of Defects in Solids", 2nd edition, Martinis Nijhoff, 1987.
5. R. M. Christensen, "Mechanics of Composite Materials", John Wiley, 1979.
6. S. P. Chen, R. LeSar and A. D. Rollett, Scr. Met. et Mat., **28**, 1393 (1993).
7. S. P. Chen, J. Mater. Res., submitted; S. P. Chen, R. LeSar and A. D. Rollett, Mater. Res.
Soc. Proc. **322**, 229 (1994).
8. S. P. Chen, Scripta Met. et Mat., **31**, 1437 (1994) and to be published.
9. L. Monette and M. P. Anderson, Scr. Met. et Mat., **28**, 1095 (1993); L. Monette, M. P.
Anderson, G. S. Grest, J. Appl. Phys., **75**, 1155 (1994); L. Monette, M. P. Anderson, H.
D. Wagner, R. R. Mueller, J. Appl. Phys., **75**, 1442 (1994).
10. A. Jagota and G. W. Scherer, J. Am. Ceram. Soc., **76**, 3123 (1993); A. Jagota and S. J.
Bennison, in " Breakdown and non-linearity in soft condensed matter", ed. by K. K.
Bardhan, B. K. Chakrabarti and A. Hansen, Springer Verlag, Berlin, to be published.
11. M. Y. He and J. W. Hutchinson, Int. J. Solids Structures, **25**, 1053 (1989).
12. D. L. Tullock, I. E. Reimanis, A. L. Graham and J. J. Petrovic, Acta Met. et Mat., in
press.
13. D. Marshall and A. G. Evans, J. Am. Ceram. Soc., **68**, 225 (1985).
14. D. C. Phillips, J. Mater. Sci., **7**, 1175 (1972).
15. E. Bischoff, O. Sbaizero, M. Ruhle, and A. G. Evans, J. Am. Ceram. Soc., **72**, 741 (1989).
16. H. Kung, R. G. Castro, A. Bartlett, and J. J. Petrovic, to be published.

17. S. P. Chen, Phil. Mag. A, **66**, 1 (1992).